Bioorganic & Medicinal Chemistry 18 (2010) 8270–8276

Contents lists available at ScienceDirect

Bioorganic & Medicinal Chemistry

journal homepage: www.elsevier.com/locate/bmc

Zinc-finger hydrolase: Computational selection of a linker and a sequence towards metal activation with a synthetic αββ protein

Kirti Patel [†], Kinshuk Raj Srivastava, Susheel Durani [*]

Department of Chemistry, Indian Institute of Technology Bombay, Mumbai 400 076, India

ARTICLE INFO

Article history:
Received 23 August 2010
Revised 30 September 2010
Accepted 2 October 2010
Available online 27 October 2010

Keywords:
Protein design
Zinc-binding sites
Protein stereochemistry
Enzyme-catalysis
Cholinesterase
π–π interactions

ABSTRACT

The zinc-finger protein is targeted for computational redesign as a hydrolase enzyme. Successful in having zinc activated for hydrolase function, the study validates the stepwise approach to having the protein tuned in main-chain structure stereochemically and over side chains chemically. A leucine homo-polypeptide, harboring histidines to tri coordinate zinc and D-amino-acid-nucleated α-helix and β-hairpin building blocks of an αββ protein, is taken up for modeling, first with CYANA, in a mixed-chirality linker between the building blocks, and then with IDeAS, in a sequence over side chains. The designed mixed-chirality polypeptide structure is proven to order as an intended αββ fold and capture zinc to activate its role as a hydrolase catalyst. The design approach to have protein folds defined stereochemically and receptor and catalysis functions defined chemically is presented, and illustrates L- and D-α-amino-acid structures as the alphabet integrating chemical- and stereochemical-structure variables as its letters.

1. Introduction

Proteins are polypeptide structures defined in the folds, in the binding sites, and in the catalysis functions with side-chain structures as the chemical alphabet. The alphabet evokes interest of application for design of proteins and enzymes, but presents in the compounded size of conformational- and chemical-search spaces a formidable challenge. The searches can be undertaken computationally, and particularly powerful can be the approach to have the conformational-structure space in main-chain and chemical-structure space over side chains delinked and explored independently. Implementing the possibility is the inverse-design algorithm[1–6] which has been applied successfully for the design, from input of main-chain folds, of new proteins,[7] new sensors,[8] and new enzymes,[9–11] etc. The complementary methods for fold design are desired, and molecular dynamics[12] and Monte Carlo[13] procedures are the relevant methods. We have proposed the novel concept of protein design involving the use of residue stereochemistry as an additional alphabet.[14] For the designs, we have reported relevant computational methods, which may be implemented over preordered secondary structures or unordered polypeptides structures as the input.[12,14] A complementary method for design of sequences over the mixed-stereochemistry folds has also been reported.[15] Illustrating the method, we have in parallel studies reported the design of a mixed-chirality-peptide hydrolase,[16] and of a hemoglobin-like tetramer over a canonical β-hairpin structure.[17] We now aim the stepwise design of a zinc-finger hydrolase, first over main-chain and then over side-chain structures.

Hydrolase enzymes harness acid–base–nucleophile catalysts from within their polypeptide structures and electrophile catalysts as external cofactors. Zn is an important protein cofactor contributing both structural and catalysis roles.[18,19] Studies have been reported where the binding of Zn provides major driving force for a polypeptide chain to fold.[21] Zinc-finger protein,[20] having zinc tetra coordinated with an αββ fold, typifies zinc in the structural role. Zinc also contributes in enzyme-catalysis functions, and there are reports of successful modification of zinc-finger structure as a hydrolase enzyme.[22–24] Illustrating L- and D-α-amino-acid alphabet, we reported the design of small αββ protein as a binding pocket for acetylcholine, calling it pi-cup protein.[25] We now report computational modification of pi-cup-protein structure as a zinc-based hydrolase. The study illustrates the computational methods developed in our lab for implementing protein design over L- and D-α-amino-acid structures as the combined stereochemical and chemical alphabet.[12,15,16,25,26]

2. Results

2.1. Design and synthesis

We aim to have an αββ fold tri-coordinate zinc, towards metal activation as a hydrolase catalyst. Figure 1 compares zinc-finger

* Corresponding author. Tel: +91 22 25767164; fax: +91 22 25767152.
E-mail address: sdurani@iitb.ac.in (S. Durani).
† Present address: Department of Chemistry, RNC Arts, JDB Commerce & NSC Science College, Nashik Road, 422 101, India.

0968-0896/$ - see front matter © 2010 Elsevier Ltd. All rights reserved.
doi:10.1016/j.bmc.2010.10.003

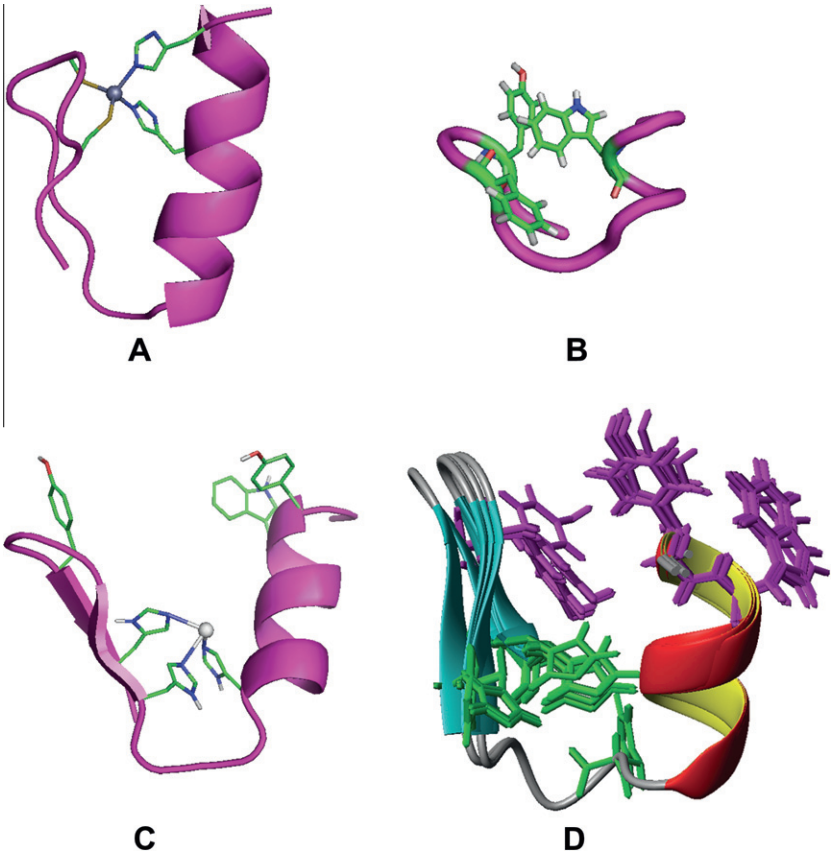

Figure 1. αββ Folds natural and synthetic. (A) Natural zinc-finger fold. (B) Synthetic pi-cup protein. (C) Zinc-finger fold modified as a potential metallo-hydrolase. (D) Ten lowest energy NMR models for the synthetic sequence obtained with CYANA

fold,[19] pi-cup protein,[25] and the synthetic transform we are aiming to achieve as an enzyme. We seek to suitably enlarge α-helix, β-hairpin, and linker elements of the pi-cup protein, and incorporate histidines to tri-coordinate zinc, placing it in the base of an intended active-site cleft. We implement the design as follows. In a 21-residue polypeptide, we place in positions 1 and 17 ^{D}Pro, in positions 10, 14, and 21 ^{L}His, in positions 11, 12, 13, and 18 Gly, and in every remaining sequence position ^{L}Leu. As reported,[26] we model an αββ fold with NMR-structure solving software CYANA.[27] Annealing proteins typically with input of NMR-derived constraints, the software can accept design constraints of interest as well as artificial residues. We have modified CYANA package by having D amino acids incorporated in its library.

We implement fold design by constraining secondary-structure elements locally and desired tertiary-structure fold globally. The constraints, imposed in form of distances between atoms or molecular fragments and torsional angles in specific elements of the structure, are allowed sufficient tolerances for plasticity of conformation and flexibility of atomic packing when implementing simulated-annealing cycles of CYANA. Specifically, for the design objective in this study, we constrained His residues of polypeptide structure to the geometry suitable for coordination with zinc.[18] Constraining intended secondary-structure modules appropriately to intended tertiary structure, we allowed tri-glycine linker to sample the possibilities of conformational space compatible with the targeted ααβ protein. Multiple runs of CYANA were followed with analysis of the folds in the conformations over the individual glycine residues in the desired ααβ protein. Over 500 annealing runs, summarized in Figure S2 of the Supplementary data, the glycines in sequence positions 11 and 13 are noted to sample more frequently either the left or the right half of φ,ψ space, suggesting the possible use in our design of L or D residue as replacements for the glycines. The glycine in sequence position 12 does not manifest preference for a specific half of φ,ψ space, and is thus retained in our final sequence design unchanged.

With the choices for the residues in the intended linker segment worked out, we took up the design of sequence with IDeAS,[15] the software developed to allow mixed chirality folds to be targeted with L or D side chains, as required. Keeping specific residues fixed, the structure was sequence optimized as the intended protein and enzyme. Specifically, $^{D}Pro_1$ was kept fixed as a nucleator for the helical fold, $^{D}Pro_{17}$-Gly_{18} was kept fixed as a nucleator for the Type-II' β-hairpin, $^{L}His_{10}$, $^{L}His_{14}$, $^{L}His_{21}$ were kept fixed as the zinc ligands, and Gly_{12} was kept fixed as a connector-segment residue, in accordance with the results of the CYANA-based analysis. Implementing IDeAS, a sequence solution was generated by having the solutions in the sequence position 11 constrained to only D residues, and in the sequence positions 2, 3, and 19 constrained only to aromatic residues. The latter are intended for the possibility of constraining the folding and ligand binding with aromatic interactions of the selected residues. Allowing in every other sequence position an unrestricted choice of side chains, the following sequence generated with IDeAS was selected as the ideal option in respect of sequence polarity and chemical diversity of the structure.

Ac^{D}Pro$_1$-Tyr$_2$-Trp$_3$-Gln$_4$-Ala$_5$-Ser$_6$-Asp$_7$-Lys$_8$-Arg$_9$-His$_{10}$-^{D}Glu$_{11}$-Gly$_{12}$-Asp$_{13}$-His$_{14}$-Ser$_{15}$-Gln$_{16}$-^{D}Pro$_{17}$-Gly$_{18}$-Tyr$_{19}$-Thr$_{20}$-His$_{21}$NH$_2$

The sequence describes an αββ fold tri-coordinating zinc, as noted in Figure 1C. Compared with the zinc-finger[20] and pi-cup proteins,[25] the designed protein is extended in the linker between the α-helix and β-hairpin elements, and harbors a pocket towards eventual tune-up for a desired binding ligand. The peptide was synthesized by manual solid-phase chemistry. Ion peak in

correspondence of the expected molecular mass is found to appear in MALDI–MS, as is noted in Figure S1 of the Supplementary data. HPLC over RP-C_{18} column with H_2O (0.01% TFA)–acetonitrile 0–100% gradient established that the peptide was >90% pure.

2.2. Characterization of conformation

A coupled minimum and maximum of ellipticity appears at 212 and 228 nm in CD spectrum, as is noted in Figure S3A. The bands characterize a coupled exciton, the hallmark of aromatic chromophores in mutual interaction.[28] The Tyr in sequence position 19 may be interacting with the Tyr in sequence position 2 or the Trp in sequence position 3, implying that the polypeptide has its termini in close proximity, even when it is not ligated with zinc. β-Hairpin and α-helix elements may be ordered, but the characteristic minima of CD, expected in the range of ~208–235 nm, cannot be observed, possibly due to the strength of the coupled exciton. As evidence for a chirally perturbed aromatic group, the peptide displays a CD band in 260–350 nm range, as is noted in Figure S3B of the Supplementary data. The peptide is in its molar ellipticity concentration invariant in the 20–100 μM regime, as is noted in Figure S3A of the Supplementary data. Presumably, the peptide is a monomolecular fold aggregation free in the concentration regime examined.

Table 1
Proton chemical shifts

Residue	NH	CαH	CβH	CγH	Others
Pro-1		4.29	2.07, 1.86	1.70, 1.51	3.525
Tyr-2	8.01	4.63	3.05, 2.97		7.49, 6.84
Trp-3	8.07	4.17	3.26, 3.21		7.22, 10.11, 7.54, 7.21, 7.46, 7.11
Gln-4	8.37	4.17	1.79, 1.70	1.66, 1.41	7.44, 6.81
Ala-5	8.18	4.19	1.38		
Ser-6	8.53	4.50	3.83		
Asp-7	8.13	4.49	2.77, 2.69		
Lys-8	8.43	4.24	1.74	1.54	1.69, 3.10, 7.35
Arg-9	7.95	4.15	1.95, 1.79	2.11, 2.18	3.24, 3.20, 7.39, 6.76
His-10	8.07	4.57	2.94, 2.74		8.02, 7.51
Glu-11	8.44	4.67	2.07, 1.91	2.33, 2.32	
Gly-12	8.40	3.88			
Asp-13	7.82	4.51	2.75, 2.64		
His-14	8.12	4.63	3.21		7.57, 7.20
Ser-15	8.22	4.45	3.87		
Gln-16	8.08	4.17	1.96, 1.80	2.20, 2.14	7.05, 6.75
Pro-17		4.38	2.26, 1.98	1.86	3.75, 3.67
Gly-18	8.29	3.83			
Tyr-19	7.97	4.60	3.01, 2.94		6.94, 6.73
Thr-20	8.13	4.30	4.09	1.10	
His-21	8.32	4.62	3.21, 3.08		7.16, 6.82

^{1}H NMR spectrum recorded in 90:10 H_2O/D_2O mixture at pH 6.7 is well dispersed in chemical shifts, and is unaffected by dilution of the peptide from 3 mM and 0.3 mM concentration, as is noted in Figure S4 of the Supplementary data. Apparently, the peptide is free of aggregation in the concentration regime of NMR experiment as well. Chemical shift assignments were achieved with TOCSY[29] and NOESY.[30] Portions of 2D spectra are shown in Figures S5–S7 of the Supplementary data. Chemical shift assignments are given in Table 1. Deviations of CαH shifts from random-coil values, called CSI, is a useful diagnostic of secondary structure.[31,32] The CSIs in our peptide, noted in Figure 2, are in accordance with the expectation for its α-helical fold but not for its β-hairpin fold. Arising locally from peptide-dipolar fields, CSIs are known to diminish in proportion of the access a peptide has to solvent.[33] Hence, small in size, the peptide may not conform to the CSIs derived from proteins. $^3J_{NHC\alpha H}$ values, as could be read off from 1D spectrum, are listed in Table 2. With $^3J_{NHC\alpha H} \leqslant 3.2$ Hz, Tyr(2), Ser(6), Asp(7), Lys(8), and His(10) evidently are in α-helical conformation, while with $^3J_{NHC\alpha H} \geqslant 8$ Hz, His(14), Ser(15), and Gln(16) evidently are in β-sheet conformation.[30]

Rich population of NOEs appeared in NOESY, implying short contacts between several residues possibly far off in sequence. As noted in Figures 3 and 4 and Figure S7 of the Supplementary data, NOEs appear between the main-chain protons of Gln(16)-Tyr(19), Ser(15)-Thr(20), and His(14)-His(21), in support of β-hairpin fold, of Gln(4)-Asp(7), Gln(4)-Lys(8), Ser(6)-His(10), and Ala(5)-Arg(9), in support of α-helical fold, and between the side-chain protons of Tyr(2)-Tyr(19), Trp(3)-Tyr(19), Gln(16)-Trp(3), and Gln(16)-Arg(9), in support of αββ fold of the protein.

Modeling with CYANA 2.1,[27] using 128 NOE-calibrated distance restraints (76 intra residue, 31 medium, and 21 long range) and 11 $^3J_{NHC\alpha H}$-calibrated φ restraints, led to convergence of the peptide as an αββ fold. The 10 best-fit conformers, superposed in Figure S1D of the Supplementary data, are in mutual global root-mean-square deviation (RMSD) over backbone atoms, excluding N- and C-terminal residues, of 0.26 ± 0.27 Å. The structures are with side chains of Tyr(2), Trp(3), and Tyr(19) in close enough proximity for NH-π, CH-π, and π–π interactions.

2.3. Binding with Zn^{2+}

Evaluation of Zn^{2+} binding was undertaken with MALDI-MS, NMR, CD, and Isothermal Titration Calorimetry (ITC). In MALDI–MS recorded in the presence of 10-fold excess of $Zn(ClO_4)_2{\cdot}6H_2O$, shown in Figure S8 of the Supplementary data, ion peak appears in correspondence of Zn^{2+}-peptide complex in stoichiometry of 1:1. In NMR, a slight perturbation occurs on addition of $Zn(ClO_4)_2{\cdot}6H_2O$ in 5 mol excess, but only in NH region, as is noted

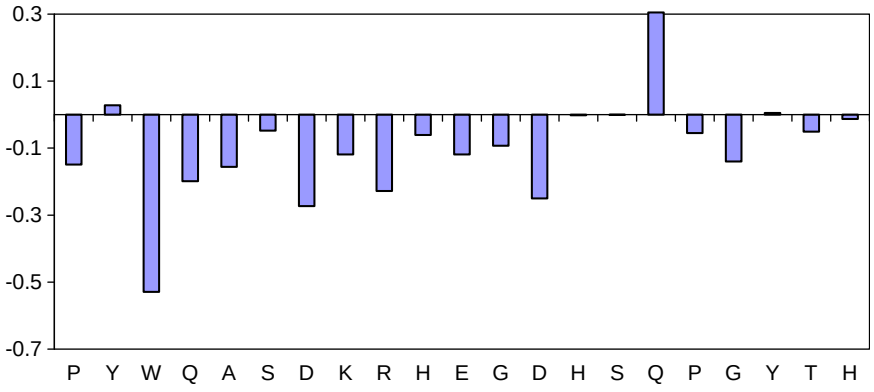

Figure 2. Deviations of observed CαH chemical shifts ($\Delta\delta H\alpha$) from mean random-coil values.

Table 2
$^{3}J_{NHC\alpha H}$ values

Residue	$^{3}J_{NHC\alpha H}$ (Hz)
Tyr(2)	3.20
Ser(6)	2.80
Asp(7)	2.80
Lys(8)	2.40
His(10)	2.40
Asp(13)	7.20
His(14)	8.00
Ser(15)	8.00
Gln(16)	8.00
Tyr(19)	7.20
His(21)	7.20

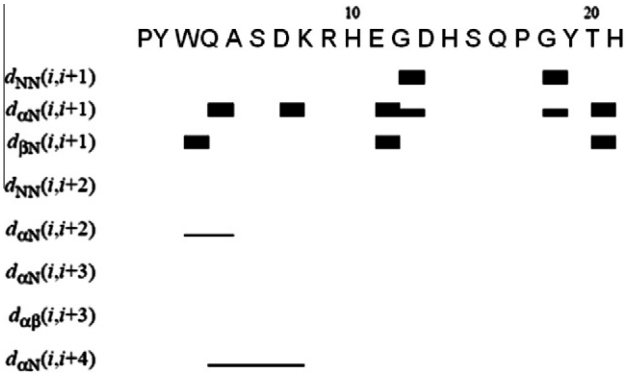

Figure 3. Near neighbor backbone NOEs of αββ fold.

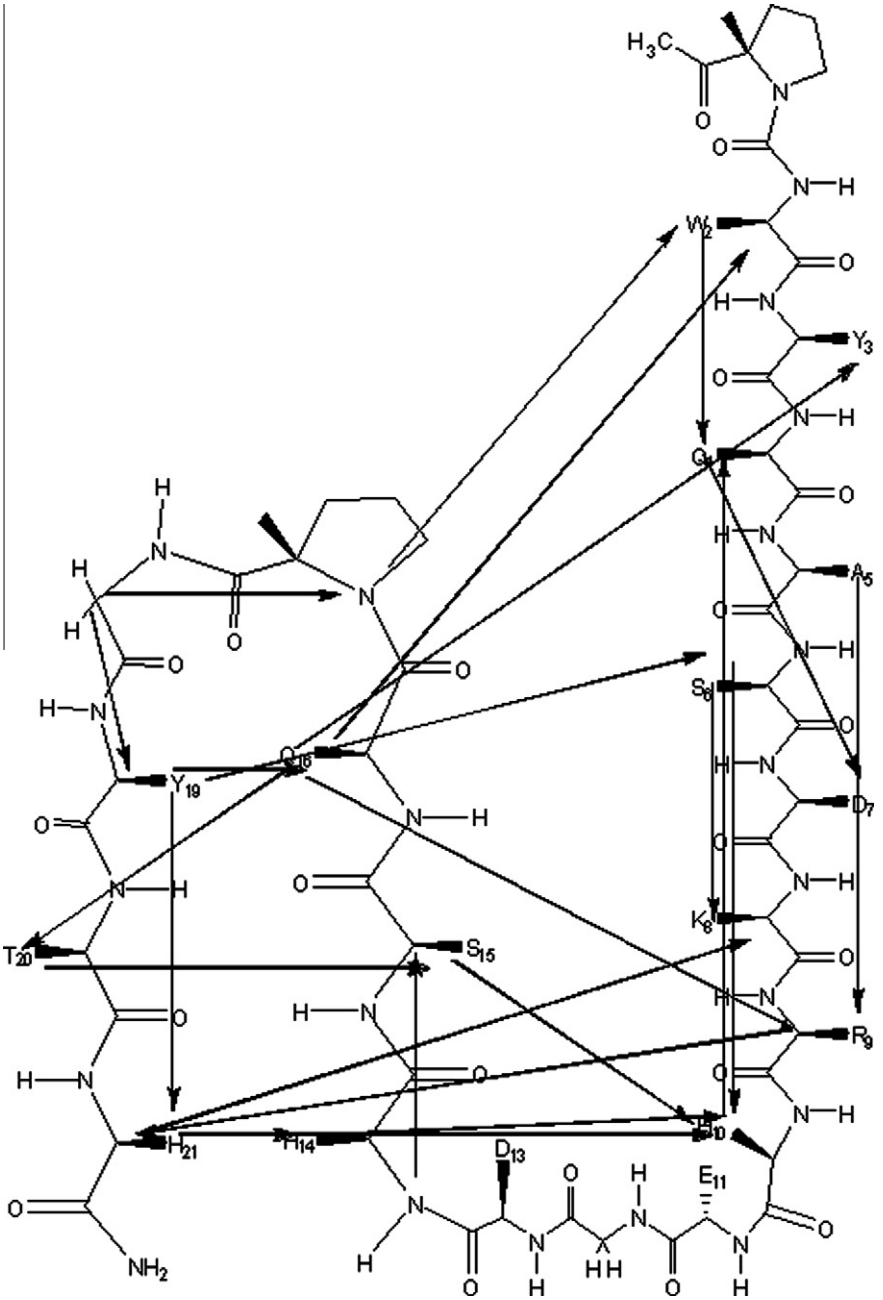

Figure 4. Schematic representations of long range NOEs of αββ fold.

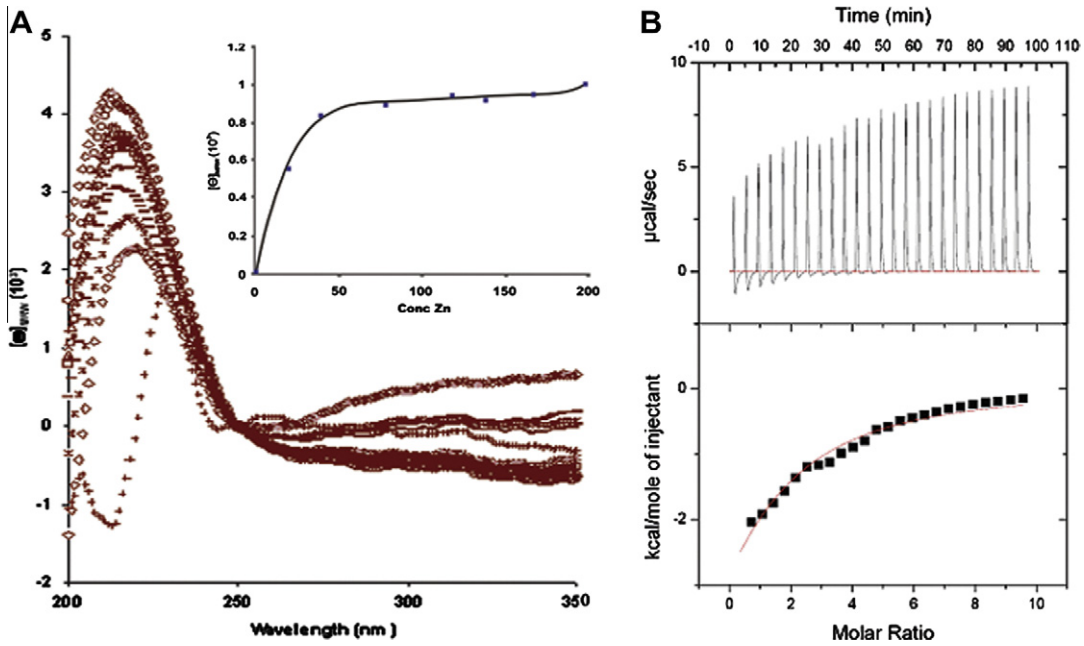

Figure 5. (A) Concentration-dependent perturbation of exciton-coupled CD band of peptide with Zn^{2+}, (inset) the dependence of ellipticity at 212 nm on concentration of zinc. (B) Microcalorimetric evaluation of peptide–Zn^{2+} interaction. Upper panel: measured heat change on adding aliquots of $Zn(ClO_4)_2$ into peptide solution. Lower panel: integrated heat change in each step with solid line in correspondence of single-site binding model.

in Figure S9 of the Supplementary data. Presumably, the peptide is preordered to the zinc-binding conformation. Titration with Zn^{2+} leads to perturbation of exciton-coupled CD band of the peptide, affecting its ellipticity at 212 nm. Monitoring zinc interaction with CD and fitting the data to 1:1 isotherm, gave K_d as 874 ± 360 µM and correspondingly ΔG° as −16.5 kJ mol^{-1}. The interaction could be monitored with ITC as well. According to the results given in Figure 5B, the interaction is saturable and exothermic. Parameters derived from the titration, by assuming 1:1 isotherm, are given in Table 3. K_d of 716 ± 55 µM, and correspondingly ΔG° of −17.9 kJ mol^{-1} are in agreement with the results of CD experiment.

Table 3
Thermodynamic parameters for peptide–Zn^{2+} interaction derived with CD and ITC

	ΔH° (kJ/mol)	ΔS° (J/mol)	K_d (µM)	ΔG° (kJ/mol)
ITC	−50.87 ± 1.80	−26.41	716.40 ± 55.55	−17.93 ± 0.04
CD	—	—	873.97 ± 359.69	−16.51 ± 1.12

2.4. Evaluation of catalysis

The peptide was evaluated as a hydrolase against *p*-nitrophenylacetate (pNPA) as the acetylcholine surrogate. Hydrolysis of the substrate with only zinc, with only peptide, and with Zn–peptide

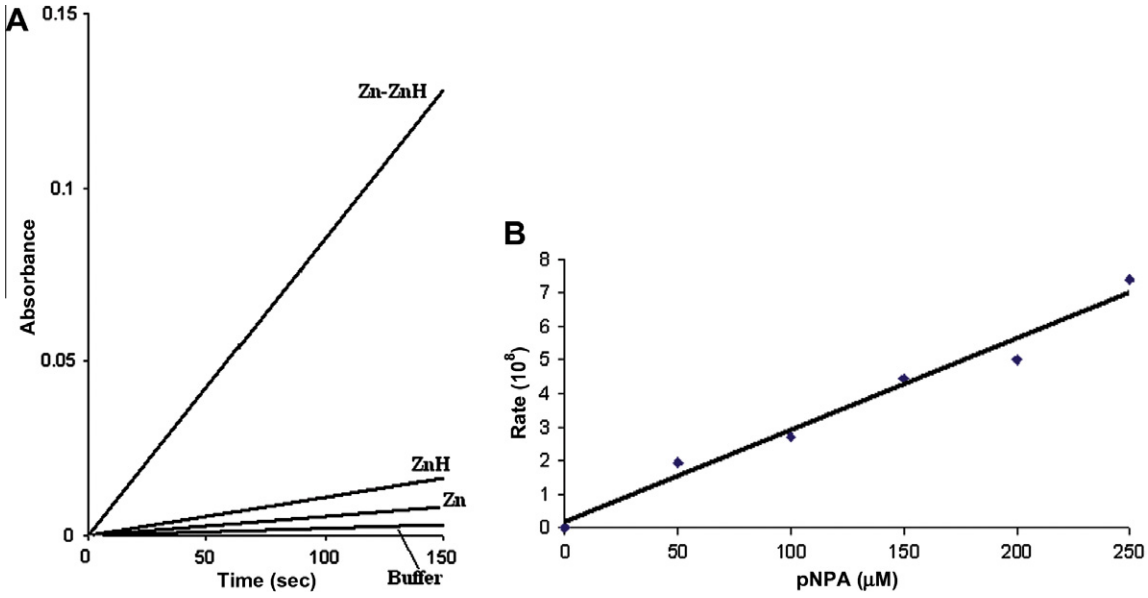

Figure 6. (A) UV monitored rate of hydrolysis of pNPA in buffer showing effects of added $Zn(ClO_4)_2$, free peptide, and Zn–peptide complex. (B) Rate of hydrolysis of pNPA with Zn–peptide complex (1 µM peptide + 5 µM Zn^{2+}) as a function of substrate concentration.

Table 4
Initial rate (v) for hydrolysis of pNPA

Catalyst	v (10^{-9} Ms^{-1})	v/v_{contr}[a]
Buffer	2.30 ± 0.03	1.00
Zn	5.75 ± 0.03	2.5
Peptide	11.49 ± 0.21	4.99
Zn–peptide	103.45 ± 0.25	44.98

[a] Rate of hydrolysis of pNPA by buffer was taken as v_{contr}.

complex is plotted in Figure 6 A and the derived rate constants are summarized in Table 4. Small rate enhancement occurs with only zinc and with only the peptide, while a ~45-fold rate enhancement occurs with the zinc–peptide complex. The results in Figure 6B show that the hydrolysis rate does not saturate with the substrate concentration. Michaelis–Menten model is ruled out and the hydrolysis with zinc–peptide complex may involve collisional mechanism rather than a specific complexation between the substrate and the enzyme.

3. Discussion and conclusions

The protein alphabet of α-amino-acid structures, by now clarified to some extent in its operational physics, has begun to yield in the efforts to have it applied.[1–6] Algorithms developed for its application[12,13] have been validated with the successful design of proteins,[2,15] receptors,[20] sensors,[8] and enzymes.[9–11] The algorithms work by delinking the search space of the structure in sequences over side chains from that of conformational folds over main-chain. The development motivates the exploration of fold design with the recruitment of possible newer variables of structure. We have proposed and explored residue chirality as a variable for fold design,[14] and have reported the computational methods suitable for sampling and exploring mixed-L,D-polypeptide structures in their diversity of folds,[12] for having the folds evaluated in fitness to be designable as proteins,[34] and for having main-chain folds optimized for possible desired application over the chemical alphabet in side chains.[15] To test the methods,[15,25] the present study aimed the computational reprogramming of zinc-finger protein as a hydrolase enzyme. While protein design field has witnessed improvements in the force fields,[35,36] the search size of conformational structures and sequence over side chains remains prohibitive and the reason protein-structure prediction from input of sequence remains a challenge largely usolved.[37] The design field has advanced by having the sequence design and the conformational design delinked.[3–5] Leveraging the delinking, we have reported independent methods for design first over the stereochemical alphabet in L and D structure and then over the chemical alphabet in side chains.[14]

The catalysis function in metal-hydrolases involves the side chains in a multitude of roles, including the coordination with metal ion and its activation as a hydrolase. Here we have approached the activation of zinc in a possible zinc-finger-like αββ protein. The design of a linker to join D-amino-acid nucleated secondary structures was implemented with CYANA.[26] Several software have been developed for inverse optimizing folds,[2] and we have developed IDeAS to have side chains applied to hetero-chiral folds in the chirality of interest.[15] Applying first CYANA and then IDeAS, an αββ protein was achieved as a Zn-based hydrolase in this study. The coordination and activation of zinc as a hydrolase catalyst was achieved successfully but not the binding of the substrate and its enzyme-like hydrolysis. Design of a metal-free hydrolase, illustrating rational approach to the modeling of folds over the alphabet in L and D structures, is reported elsewhere.[16] Future iterations of the structure accomplished in the present study will aim to find and tune the determinants of its affinity for zinc and its further development as an enzyme.

4. Experimental section

4.1. Materials

p-Nitrophenylacetate and $Zn(ClO_4)_2{\cdot}6H_2O$ were from Sigma–Aldrich. Fmoc-protected amino acids, reagents for solid-phase peptide synthesis, Rink-Amide AM resin, DMF, methanol, diethylether, dichloromethane, were from Sigma–Aldrich or Novabiochem-Merck.

4.2. Peptide synthesis

Synthesis was performed on Rink Amide AM resin using standard Fmoc chemistry and HOBt/DIC as coupling reagents. Each coupling, monitored with Kaiser and chloranil tests, typically required about 6 h. Deprotections were carried out with 30% (v/v) piperidine-DMF. N-Terminus was acetylated ($-NHCOCH_3$) with Ac_2O/DIPEA/DMF in 1:2:20 ratio. The cleavage of the final polypeptide and deprotection of side chains were achieved together with reagent K (82.5% TFA/5% dry-phenol/5% thioanisole/2.5% ethandithiol/5% water). The product precipitated with anhydrous diethyl ether was lyophilized from 1:4 H_2O/^{t}BuOH solution as a white powder. Peptide purity was assessed with HPLC over RP-C18 (10 μM, 10 mm × 250 mm; Merck) eluting with CH_3CN/H_2O (0.1% TFA) 0–100% gradients.

4.3. Mass spectra

Mass spectra were recorded in MALDI-TOF (Matrix Assisted Laser Desorption Ionization-Time of Flight) mode or on AXIMA-CFR Kratos instrument.

4.4. Circular dichroism

Circular dichroism (CD) was recorded on JASCO J-180 CD spectropolarimeter at 298 K in 0.2 cm path length quartz cell with 2 nm bandwidth in far-UV (190–250 nm) or near-UV (250–350 nm) range. Scanning at 100 nm/min with 1.0 s time constant, in 1 nm steps, five scans were averaged after baseline correction for solvent. Working solutions 20–100 μM in peptide were prepared by optical measurements and of $Zn(ClO_4)_2{\cdot}6H_2O$ gravimetrically. The observations in millidegrees were converted to molar residue ellipticity [θ_{MRW}] with a reported relation.[38]

4.5. Nuclear magnetic resonance

^{1}H NMR was on Bruker 800 MHz spectrometer, equipped with cryoprobe, at 298 K. Peptide concentrations of 3 mM were used, and 1D spectra were recorded also at 10-fold dilution. Solutions were prepared in 90% H_2O/10% D_2O with DSS as the internal reference at pH 6.7 in presence and absence of Zn. Polypeptide backbone and side-chain assignments were obtained with 2D ^{1}H–^{1}H TOCSY[28] experiments using standard mlevtp pulse sequence for spin lock. Spin lock time of 80 ms was used to ensure observation of long-range couplings. The data were collected in 2 k time domain points. 512 increments of t_1 were measured with 48 FIDs per increment, the data being zero-filled to 1 k data points in F_1 prior to Fourier transform. Distance constraints were obtained from a 2D ^{1}H–^{1}H NOESY experiment[29] with mixing time of 300 ms. The data were processed with TOPSPIN 2.0 and 2.1 and analyzed with Computer Aided Resonance Assignment (CARA) software. Structure calculations were performed with CYANA 2.1.[27]

Dihedral angle restraints based on $^{3}J_{NHC\alpha H}$ values were used, wherever possible, for structure refinements. D-Amino acid residues were introduced in CYANA library under the guidance of the developer. Structures were energy minimized using GROMACS software package.[39] Structural models were rendered with PYMOL, MOLMOL or VIEWERLITE softwares.

4.6. Isothermal titration calorimetry (ITC)

The experiments were performed on a VP-ITC micro calorimeter (Microcal, Inc.) at 298 K. Sample cell (1.448 mL) contained peptide in 100 μM concentration, as determined by optical measurement, and reference cell contained water. The 5 mM $Zn(ClO_4)_2{\cdot}6H_2O$ (ligand) solution loaded in 250μL syringe was titrated into peptide solution in 10 μL aliquots in 25 steps at 4 min intervals. The change in enthalpy (ΔH) due to dilution was determined by titrating ligand into solvent as well as solvent into peptide solution. These backgrounds were subtracted from ΔH obtained for the corresponding ligand–peptide binding experiments, prior to curve fitting. The background-subtracted data was fitted to a model describing single binding site using MicroCal software. The binding enthalpy (ΔH), entropy (ΔS), and dissociation (K_d) constant were thus calculated.

4.7. Enzyme activity

The kinetics of hydrolysis was monitored spectrophotometrically on a Perkin–Elmer spectrophotometer, fitted with peltier, using *p*-nitrophenylacetate (pNPA) as substrate, by observing the production of *p*-nitrophenolate anion at 410 nm. Stock solution of pNPA was prepared in 20 mM sodium phosphate buffer, pH 7.0 with few drops of acetonitrile added to solubilize pNPA. Peptide concentration in the assays was in 1–10 μM range with zinc in 5 mol excess. Hydrolase activity was evaluated in 20 mM sodium phosphate buffer, pH 7.0, at 25 °C, by varying substrate concentration. The catalyzed rate of pNPA hydrolysis was measured by an initial slope method, following the increase in 410 nm absorption of *p*-nitrophenolate. Errors in observation were about 5%.

Acknowledgments

We acknowledge DST (09DST028), Government of India, for financial support. We acknowledge Professor Nand Kishore for their help with ITC experiments. K.R.S. is recipient of fellowships from Council of Scientific and Industrial Research (CSIR). We acknowledge TIFR, Mumbai for the help with NMR experiments.

Supplementary data

Supplementary data associated with this article can be found, in the online version, at doi:10.1016/j.bmc.2010.10.003.

References and notes

1. Butterfoss, G.; Kuhlman, B. *Annu. Rev. Biophys. Biomol. Struct.* **2006**, *35*, 49.
2. Das, R.; Baker, D. *Annu. Rev. Biochem.* **2008**, *77*, 363.
3. Lippow, S.; Tidor, B. *Curr. Opin. Biotechnol.* **2007**, *18*, 1.
4. Park, S.; Yang, S.; Saven, J. *Curr. Opin. Struct. Biol.* **2004**, *14*, 487.
5. Dahiyat, B. I.; Mayo, S. L. *Protein Sci.* **1996**, *5*, 895.
6. Dahiyat, B. I.; Sarisky, C. A.; Mayo, S. L. *J. Mol. Biol.* **1997**, *273*, 789.
7. Kuhlman, B.; Dantas, G.; Ireton, G. C.; Varani, G.; Stoddard, B. L.; Baker, D. *Science* **2003**, *302*, 1364.
8. Allert, M.; Rizk, S.; Looger, L.; Hellinga, H. *Proc. Natl. Acad. Sci. U.S.A.* **2004**, *101*, 7907.
9. Arnold, F. H. *Nature* **2001**, *409*, 253.
10. Bolon, D. N.; Mayo, S. L. *Proc. Natl. Acad. Sci. U.S.A.* **2001**, *98*, 14274.
11. Chevalier, B. S.; Koertemme, T.; Chadsey, M. S.; Baker, D.; Monnat, R., Jr.; Stoddard, B. L. *Mol. Cell* **2002**, *10*, 895.
12. Ramakrishnan, V.; Ranbhor, R.; Durani, S. *Biopolymers* **2005**, *78*, 96.
13. Nanda, V.; DeGrado, W. F. *J. Am. Chem. Soc.* **2006**, *128*, 809.
14. Durani, S. *Acc. Chem. Res.* **2008**, *41*, 1301.
15. Ranbhor, R.; Tendulkar, A.; Kumar, A.; Ramakrishnan, V.; Patel, K.; Durani, S. Submitted for publication.
16. Patel, K.; Goyal, B.; Kumar, A.; Kishore, N.; Durani, S. Submitted for publication.
17. Pednekar, D.; Mantri, S.; Ghosh, P.; Patel, K.; Durani, S. Submitted for publication.
18. Patel, K.; Kumar, A.; Durani, S. *Biochim. Biophys. Acta—Protein Proteomics* **2007**, *1774*, 1247.
19. Berg, J. M.; Shi, Y. *Science* **1996**, *271*, 1081.
20. Lee, M. S.; Gippert, G. P.; Soman, K. V.; Case, D. A.; Wright, P. E. *Science* **1989**, *245*, 635.
21. Tang, J.; Kang, S.-G.; Saven, J. G.; Gai, F. *J. Mol. Biol.* **2009**, *389*, 90.
22. Nomura, A.; Sugiura, Y. *Inorg. Chem.* **2004**, *43*, 1708.
23. Nomura, A.; Sugiura, Y. *J. Am. Chem. Soc.* **2004**, *126*, 15374.
24. Negi, S.; Imanishi, M.; Matsumoto, M.; Sugiura, Y. *Chem. Eur. J.* **2008**, *14*, 3236.
25. Rana, S.; Kundu, B.; Durani, S. *Biopolymers* **2007**, *87*, 231.
26. Joshi, S.; Rana, S.; Wangikar, P.; Durani, S. *Biopolymers* **2006**, *83*, 122.
27. Guntert, P.; Mumenthaler, C.; Wuthrich, K. *J. Mol. Biol.* **1997**, *273*, 283.
28. Cochran, A. G.; Skelton, N. J.; Starovasnik, M. A. *Proc. Natl. Acad. Sci. U.S.A.* **2001**, *98*, 5578.
29. Davis, D. G.; Bax, A. *J. Am. Chem. Soc.* **1985**, *107*, 2820.
30. Kumar, A.; Ernst, R. R.; Wuthrich, K. *Biochem. Biophys. Res. Commun.* **1980**, *95*, 1.
31. Wishart, D. S.; Sykes, B. D.; Richards, F. M. *Biochemistry* **1992**, *31*, 1647.
32. Wishart, D. S.; Sykes, B. D.; Richards, F. M. *J. Mol. Biol.* **1991**, *222*, 311.
33. Avbelj, F.; Kocjan, D.; Baldwin, R. L. *Proc. Natl. Acad. Sci. U.S.A.* **2004**, *101*, 17394.
34. Fersht, A. R. *Structure and Mechanism in Protein Science: A Guide to Enzyme Catalysis and Protein Folding*; W. H. Freeman and Company: New York, 1998.
35. Ranbhor, R.; Kumar, A.; Patel, K.; Ramakrishnan, V.; Durani, S. Submitted for publication.
36. Mu, Y.; Kosov, D. S.; Stock, G. *J. Phys. Chem. B* **2003**, *107*, 5064.
37. Todorova, N.; Legge, F. S.; Treutlein, H.; Yarovsky, I. *J. Phys. Chem. B* **2008**, *112*, 11137.
38. Dill, K. A.; Ozkan, S. B.; Shell, M. S.; Weikl, T. R. *Annu. Rev. Biophys.* **2008**, *37*, 289.
39. Lindahl, E.; Hess, B.; van der Spoel, D. *J. Mol. Model.* **2001**, *7*, 306.